FEBS Letters 445 (1999) 402–408 FEBS 21632

Expression and a role of functionally coupled P2Y receptors in human dendritic cells

Q.H. Liu[1,a], H. Bohlen[1,b], S. Titzer[b], O. Christensen[b], V. Diehl[b], J. Hescheler[a], B.K. Fleischmann[a,*]

[a]*Institute of Neurophysiology, University of Cologne, Robert-Koch-Str. 39, D-50931 Cologne, Germany*
[b]*Department of Internal Medicine I, University of Cologne, Robert-Koch-Str. 39, D-50931 Cologne, Germany*

Received 22 December 1998; received in revised form 26 January 1999

Abstract We investigated the physiology and function of P2Y receptors expressed in human dendritic cells (DCs) differentiated in vitro from $CD14^+$ cells (DC-14). These were obtained after a 10 day stimulation period in GM-CSF, IL-4 and monocyte conditioned medium. DC-14 were found to express high amounts of MHC class II, B7, CD40 as well as CD83. The functional analysis, using single cell Ca^{2+} imaging, demonstrated the expression of at least three subtypes of P2Y receptors. We further found using patch-clamp measurements that ATP evoked a pertussis toxin insensitive non-selective cation current with a peak current amplitude of -276 ± 43 pA (holding potential -80 mV, $n = 23$). This current was not Ca^{2+}-activated, since it was still observed under conditions of high intracellular Ca^{2+} buffering and could be blocked by Gd^{3+} (0.5 mM). In addition, intracellular application of GTP-γ-S (0.3 mM) also activated the current. Interestingly, DC-14 redirected the orientation of their dendrites as well as cell shape towards a pipette containing ATP as observed with time lapse microscopy. These data suggest that in human DCs, ATP acts via P2Y receptors and induces chemokine effects.

Key words: Human dendritic cell; P2Y receptor; Non-selective cation current; Chemokine

1. Introduction

Dendritic cells (DCs) are known as the most competent and efficient cells to induce primary and secondary immune reactions. The distribution pattern of DCs ranges from primary lymphatic organs in which the phenotype is known as FDC to skin derived DCs known as Langerhans cells [1]. It is common knowledge that DCs exhibit enormous capacities to present tumorigenic antigenic peptides in both class I [2,3] and class II restricted immune responses and so far, detailed insight has been gained mainly into aspects of antigen processing and presentation [4–6]. Relatively little is known about the chemotactic events and the involved signaling mechanisms leading to DC recruitment. Whereas the uptake of soluble antigens or immune complexes can be explained by FC-mediated pathways [7–9], the recognition of antigens derived from necrotic or apoptotic cells is still under discussion. Since ATP is released from damaged cells and since purinergic receptors [10,11] are known to be expressed on a variety of immunological cells [12–17], we tested whether ATP may activate DC-14. In particular, the expression and function of purinergic receptors was studied.

We demonstrate that DC-14 express functionally coupled P2Y receptors. Extracellular application of ATP resulted in a transient increase of the free cytosolic Ca^{2+} concentration $[Ca^{2+}]_i$ and concomitant activation of a non-selective cation current. Moreover, a possible role of these purinergic receptors in ATP-mediated chemotaxis is suggested.

2. Materials and methods

2.1. DC generation

To isolate monocytes from peripheral blood, CD14 expressing cells were positively enriched using CD14 coupled paramagnetic microbeads (Miltenyi Biotech, Bergisch Gladbach, Germany) and the MiniMACS separation system (Miltenyi Biotech) according to the recommended protocol. Cells were cultured in RPMI 1640, supplemented with glutamax I (Gibco, BRL, Gaithersburg, MD, USA), 5% FCS (Gibco), 10 μg/ml ciprofloxacin (Ciprobay, Bayer, Leverkusen, Germany) containing GM-CSF (Sigma, Deisenhofen, Germany) (800 U/ml) and IL-4 (Essex Pharma, Munich, Germany) (1000 U/ml) in six well plates (Nunc, Wiesbaden, Germany) at a concentration of 10^6/ml for 10 days.

2.2. Cell surface marker analysis

Analysis of cell surface markers was performed by flow cytometry (FACSort, Becton Dickinson, Heidelberg, Germany). DC-14 (2×10^5) were stained for 15 min at 4°C in PBS, 0.1% BSA, 0.01% NaN_3 with 20 μl of PE, FITC or PerCP labeled monoclonal antibodies: CD1a, CD4, CD5, CD11a, CD11b, CD14, CD18, CD23, CD33, CD45RA, CD45RO, CD54, anti-HLA-DR (Becton Dickinson), CD30, CD30L, CD40, CD40L (Immunex Inc., Seattle, WA, USA), CD80, CD86 (Ancell, Bayport, MN, USA). After the staining procedure samples were washed twice in 1 ml PBS. Specific fluorescence intensity was defined by the ratio of the fluorescence intensity of the surface marker to the fluorescence intensity of the isotype control.

2.3. Single cell Ca^{2+} imaging experiments

DC-14 were kept in RPMI medium (Gibco) loaded with 0.5 μM fura-2-AM (Molecular Probes, Leiden, The Netherlands) in the incubator for 10 min, washed once with medium, centrifuged at 1000 rpm for 5 min and resuspended in RPMI. Then the cells were put into a temperature controlled recording chamber and superfused with extracellular solution for 10 min prior to starting the experiment. Monochromic excitation light (340–380 nm) was produced by a computer controlled monochromator (TIL Photonics, Munich, Germany) and coupled to the epifluorescence attachment of an inverted microscope (Axiovert 135TV, Zeiss, Germany) through a small quartz light guide. The excitation light was directed to the fluorescent objective (40×, Zeiss) via a dichroic mirror (TIL Photonics). The emitted fluorescence from the fura-2 loaded cells was imaged through a 470 nm interference filter using an intensified charge coupled device camera (Thetha, Munich, Germany) connected to the TV port of the inverted microscope. Fluorescence images (50 ms exposure time) were acquired at 0.33 Hz using the Fucal fluorescence software package (TIL Photonics). Images were displayed on-line and stored on hard disk. The

*Corresponding author. Fax: (49) (221) 478-6965.
E-mail: bkf@physiologie.uni-koeln.de

[1]Both authors contributed equally.

PII: S0014-5793(99)00161-1

analysis of the data was done off-line using the Fucal software package. Within cursor defined areas of interest paired 340/380 images were background subtracted and the ratio calculated. The absolute ratio values in the cursor defined areas were exported into Sigmaplot (Jandel Scientific, Germany) and the $[Ca^{2+}]_i$ concentration estimated, using the equation of Grynkiewicz et al. [18]. In situ calibration factors were determined in vitro on groups of cells and averaged, R_{max} (340/380 ratio) obtained in presence of 5 mM ionomycin and 10 mM Ca^{2+}, R_{min} (340/380 ratio) in presence of 5 mM ionomycin and excess EGTA, and $F380_{min}$ were determined. The values used for R_{max}, R_{min} and $F380_{min}$ were 2.6, 0.35 and 3.7, and a dissociation constant (K_d) of 224 was used.

2.4. Patch-clamp recordings

Standard whole-cell [19] and perforated patch-clamp techniques [20] were used for the recording of ion currents. Electrodes were pulled with a DMZ universal puller (DMZ, Munich, Germany) from 1.5 mm borosilicate glass capillaries (Clark Electromedical Instruments, Reading, UK), and fire-polished to resistances of 4–5 MΩ. Ionic currents were recorded using an EPC-9 patch-clamp amplifier (HEKA, Germany). Data were acquired with the Pulse/Pulse-Fit software package (HEKA). Liquid junction potentials, series resistance and cell capacitance were compensated using the internal circuit of the amplifier. For perforated patch recordings, freshly made stock solution of nystatin (50 mg/ml in dimethyl sulfoxide) was diluted to a final concentration of 150 μg/ml in pipette solution. In order to allow appropriate voltage clamp control, measurements were only started after the access resistance (Rs) dropped below 30 MΩ (about 5–10 min after formation of GΩ-seal). Good voltage clamp was obtained since Na^+ currents expressed in some of the DCs could be appropriately recorded.

For measurements of the instantaneous current-voltage relationship of ATP-induced currents, 150 ms ramp depolarization were applied every 1.5 s from −100 mV to 50 mV. Control currents were obtained immediately before ATP application and were subtracted from the ATP-induced current, as indicated. Continuous recordings were stored on videocassette recorder tape following pulse code modulation (VR-100A, Instrutech, Great Neck, NY, USA). Combined Ca^{2+} imaging/patch-clamp experiments were synchronized by using a TTL pulse generated by the EPC-9 to initiate the acquisition of the images. For analysis, data were downloaded from the videotape via pulse-code modulator into a software program (Axon Instruments, USA) at a sampling rate of 250 Hz and filtered at 100 Hz. Files in ASCII format were imported into Sigmaplot. Continuous observation of dendritic cells was performed using a sensitive video-camera (TIL Photonics). After the experiment videoimages were digitized and further analyzed using Adobe Photoshop software.

For electrophysiological experiments agonists were applied using a puffer pipette connected to a pressure ejection device (Picospritzer, General Valve, USA). The pipette was placed in close vicinity to the cell using a micromanipulator. For the experiments using two substances, a double barrel tubing connected to two separate perfusion pumps (Braun, Melsungen, Germany) providing steady flow rates were used. For Ca^{2+} imaging experiments reagents were applied directly to the bath or by using the double metal tubing. The total amount of ATP added is indicated in this paper. ATP was dissolved in the appropriate solution prior to use and pH corrected. The addition of 0.25 mM ATP to the normal extracellular solution yielded a free ATP concentration of 14.6 μM, whereas in the Ca^{2+} free extracellular solution free ATP was 34.5 μM as calculated with the Chelator software program (University of Nijmegen, The Netherlands).

The solutions used were of the following composition (in mM): normal extracellular solution: 140 NaCl, 4.5 KCl, 1 $MgCl_2$, 2 $CaCl_2$, 5 HEPES, pH = 7.2 (NaOH). Extracellular low Na^+ solution: 30 NaCl, 110 NMDG, 4.5 KCl, 1 $MgCl_2$, 2 $CaCl_2$, 5 HEPES, pH = 7.2 (NaOH). Extracellular low Cl^- solution: 50 CsCl, 90 Cs-acetate, 4.5 KCl, 1 $MgCl_2$, 2 $CaCl_2$, 5 HEPES, pH = 7.2 (CsOH). Extracellular Ca^{2+}-free solution: 140 NaCl, 4.5 KCl, 1 $MgCl_2$, 5 HEPES, pH = 7.2 with NaOH. Normal intracellular solution (in mM): 134 CsCl, 2 $MgCl_2$, 1 EGTA, 10 HEPES, pH = 7.2 (CsOH). Intracellular low Cl^- solution (in mM): 26 KCl, 114 K-aspartate, 2 $MgCl_2$, 1 EGETA, 10 HEPES, pH = 7.2 (KOH). All experiments were performed at room temperature (22–26°C). Gadolinium chloride (Sigma), adenosine 5′-triphosphate (ATP) (Sigma), 2-methylthioadenosine triphosphate tetrasodium (2-MeSATP, RBI, USA), guanosine 5′-triphosphate (GTP, Sigma), were dissolved in the normal extracellular solution. Guanosine 5′-*o*-(3-thiotriphosphate) (GTP-γ-S, Sigma) was dissolved in normal intracellular solution. Fura-2-AM (Molecular Probes), fura-2 pentapotassium salt (fura-acid, Molecular Probes), ionomycin (Molecular Probes) and Tg (Molecular Probes) were dissolved as stock solution in dimethyl sulfoxide (DMSO) and diluted to the final concentration prior to application (final concentration of DMSO $< 0.1\%$). Pertussis toxin (PTX) was obtained from Sigma. DC-14 were incubated in PTX (1 μg/ml) for 12 h. Averaged data are expressed as mean ± S.E.M.

3. Results and discussion

3.1. Characterization of DC-14

Using the magnetic cell separation system (MACS) for positive enrichment of CD14 expressing cells, preparations of $> 95\%$ purity were used. To obtain in vitro generated DC-14, enriched CD14 PBMC were cultured with GM-CSF/IL-4 and TNF-α (added during the last 2 days of the differentiation period) for 10 days. Expression of CD1a, CD40, CD80, CD86 and HLA-DR was strongly upregulated, as would be expected for DC-14. These show a positive staining for CD11b, CD18, CD33 and CD45RO. Two color flow cytometric analysis demonstrated a homogeneous cell population in the DC-14 with respect to cell marker distribution. After 10 days of culture in the presence of GM-CSF, IL-4 and TNFα, the DC-14 displayed a homogeneous population with DC-like features such as characteristic processes and accumulated mitochondria (data not shown). In order to characterize further the DC population the cytokine profile was analyzed by RT-PCR and ELISA at day 10 of the in vitro differentiation. It could be demonstrated that the DC-14 express a specific cytokine pattern with the presence of IL-1a, IL-1b, TNF-α, GM-CSF and the absence of IL-2, IL-4, IFN-γ at the mRNA and protein level (data not shown). Furthermore, highly purified CD4 positive autologous T cells were stimulated with the differentiated DC-14 to analyze their capacity to induce a primary and secondary antigen specific T-cell response. Within the experiments only DC-14 with a prominent antigen-presentation capacity were used.

3.2. DC-14 express functional P2Y receptors

Human CD14 derived cells were investigated at different time points (day 0–10) during differentiation using single cell Ca^{2+} imaging- and/or patch-clamp techniques. At all differentiation stages relatively linear current voltage (I/V) relationships were observed using ramp depolarization. In contrast to the findings in murine DCs [21] in the human DC-14 no inward rectifier K^+ currents and outward rectifier K^+ currents of only small amplitude were detected (data not shown). Since purinergic receptors have been detected on a variety of immunological cell types we tested the effect of extracellular application of ATP on DC-14. Using single cell Ca^{2+} imaging, ATP was found to evoke a fast, transient increase of $[Ca^{2+}]_i$ in almost all DC-14 tested (Fig. 1A, $n = 131$). A consistent response to ATP similar to terminally differentiated DC-14 was observed starting from day 5 of differentiation. The average resting $[Ca^{2+}]_i$ in DC-14 was 53 ± 2 nM and application of ATP (0.25 μM, free = 14.6 μM) resulted in peak $[Ca^{2+}]_i$ of 1001 ± 119 nM ($n = 6$). The threshold concentration of ATP for evoking a $[Ca^{2+}]_i$ transient was 0.5 μM, at this concentration, however, the peak $[Ca^{2+}]_i$ response was small (473 ± 45 nM, $n = 5$). In order to distinguish between P2X and P2Y receptors, we tested whether ATP induced Ca^{2+} release from intracellular stores. As expected for P2Y recep-

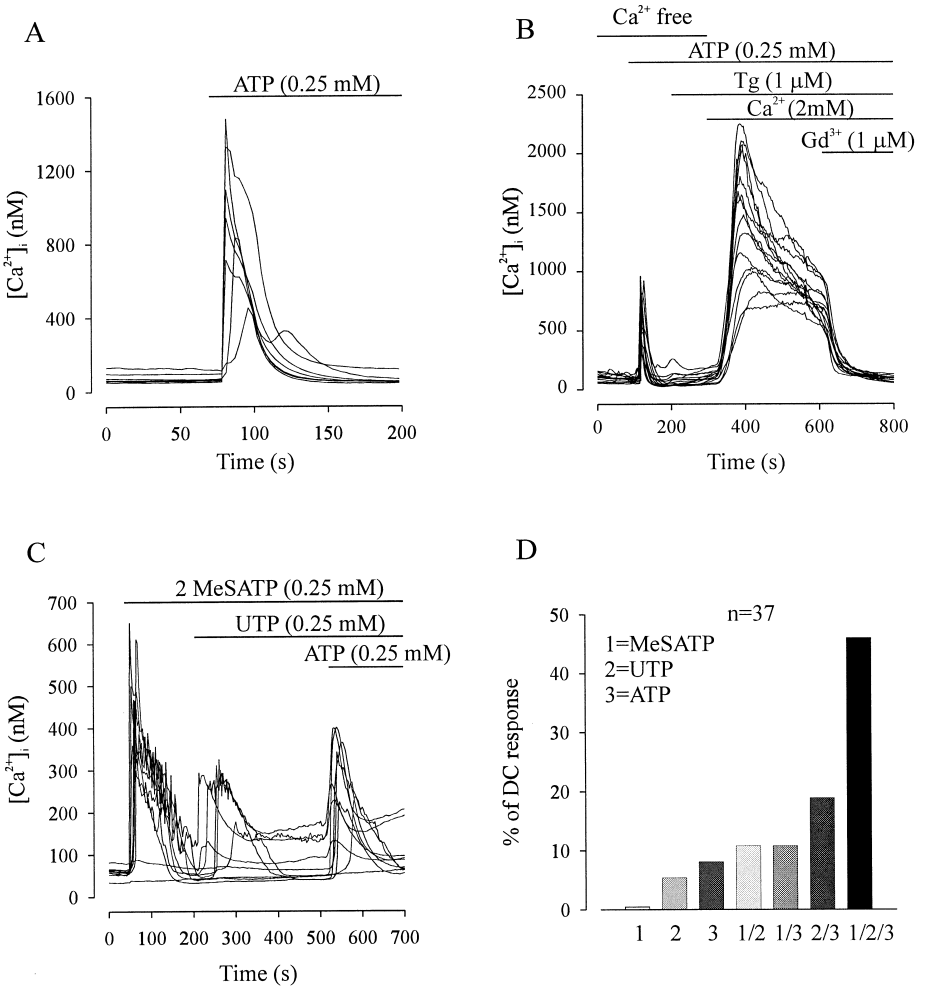

Fig. 1. ATP activates P2Y receptors in CD14 derived human DCs. A: Application of 0.25 mM ATP (free ATP = 14.6 μM) resulted in almost all DC-14 in a transient increase of $[Ca^{2+}]_i$. The magnitude of the $[Ca^{2+}]_i$ rise varied between cells, however, in all responding cells a fast return to control $[Ca^{2+}]_i$ levels was noticed. B: ATP evoked in nominally free Ca^{2+} solution (free ATP = 34.5 μM) the depletion of intracellular Ca^{2+} stores. This evidenced that the ATP response was mediated through activation of P2Y receptors. The subsequent application of Tg did not result in an additional release of Ca^{2+} from intracellular stores, excluding that the ATP action was restricted to a subclass of intracellular Ca^{2+} stores. Reperfusion with 2 mM Ca^{2+} containing extracellular solution resulted in a sustained increase of $[Ca^{2+}]_i$, which could be completely blocked by Gd^{3+} (1 μM). C: DC-14 expressed several subtypes of P2Y receptors, since the majority of cells responded with transient $[Ca^{2+}]_i$ increases to the sequential application of 2MeSATP, UTP and ATP. D: Statistics from three representative experiments where P2Y receptor agonists were applied in the same order as in C. It is shown that most of the DC-14 cells coexpressed at least three different P2Y receptor subtypes. Furthermore, it can be seen that there is variability among the human DC-14 in regard to P2Y receptor expression.

tors [10], ATP evoked a transient $[Ca^{2+}]_i$ increase in nominally Ca^{2+} free extracellular solution (Fig. 1B, $n = 150$). The ATP induced depletion of intracellular Ca^{2+} stores was further proven by Tg, a Ca^{2+}-ATPase inhibitor [22]. After application of ATP, Tg did not evoke an additional increase of $[Ca^{2+}]_i$ (Fig. 1B) in line with ATP emptying the intracellular stores. Tg evoked a sustained rise in $[Ca^{2+}]_i$ upon the readdition of extracellular Ca^{2+}, which was completely blocked by 1 μM Gd^{3+}, indicating the activation of the store depletion activated current (I_{CRAC}, Fig. 1B) [23]. In contrast, extracellular ATP caused only a transient $[Ca^{2+}]_i$ increase (Fig. 1A). In order to characterize the functionally expressed P2Y receptor subtypes [24] the P2Y1 selective agonist 2-MeSATP [25–27] (2–7) was first applied; then the P2Y2 [28,29] and P2Y4 [30,31] agonist UTP was added. As depicted in Fig. 1C, 2-MeSATP as well as UTP evoked similar to ATP a transient $[Ca^{2+}]_i$ increase in DC-14. Moreover, subsequent application of ATP in the presence of 2-MeSATP and UTP caused an additional transient $[Ca^{2+}]_i$ response in most cells suggesting the functional expression of 2-MeSATP and UTP insensitive P2Y receptors (Fig. 1C). Accordingly, the application of ATP prevented the subsequent 2-MeSATP- and UTP-induced $[Ca^{2+}]_i$ elevation (data not shown). A summary of three representative experiments where the different agonists were applied in the order 2-MeSATP-UTP-ATP demonstrated that most of the cells tested express at least three subtypes of P2Y receptors (Fig. 1D).

3.3. ATP activates a non-selective cation current in DC-14

Next, we wondered whether P2Y receptor activation was associated with changes in membrane conductance. Combined single cell Ca^{2+} imaging and perforated patch-clamp recording evidenced that ATP evoked both, the increase of $[Ca^{2+}]_i$ (Fig. 2Aa) and the activation of an inward current (Fig. 2Ab, HP = −80 mV, $n = 4$). This current was of a slowly activating and inactivating nature. As depicted in Fig. 2Aa/b the increase

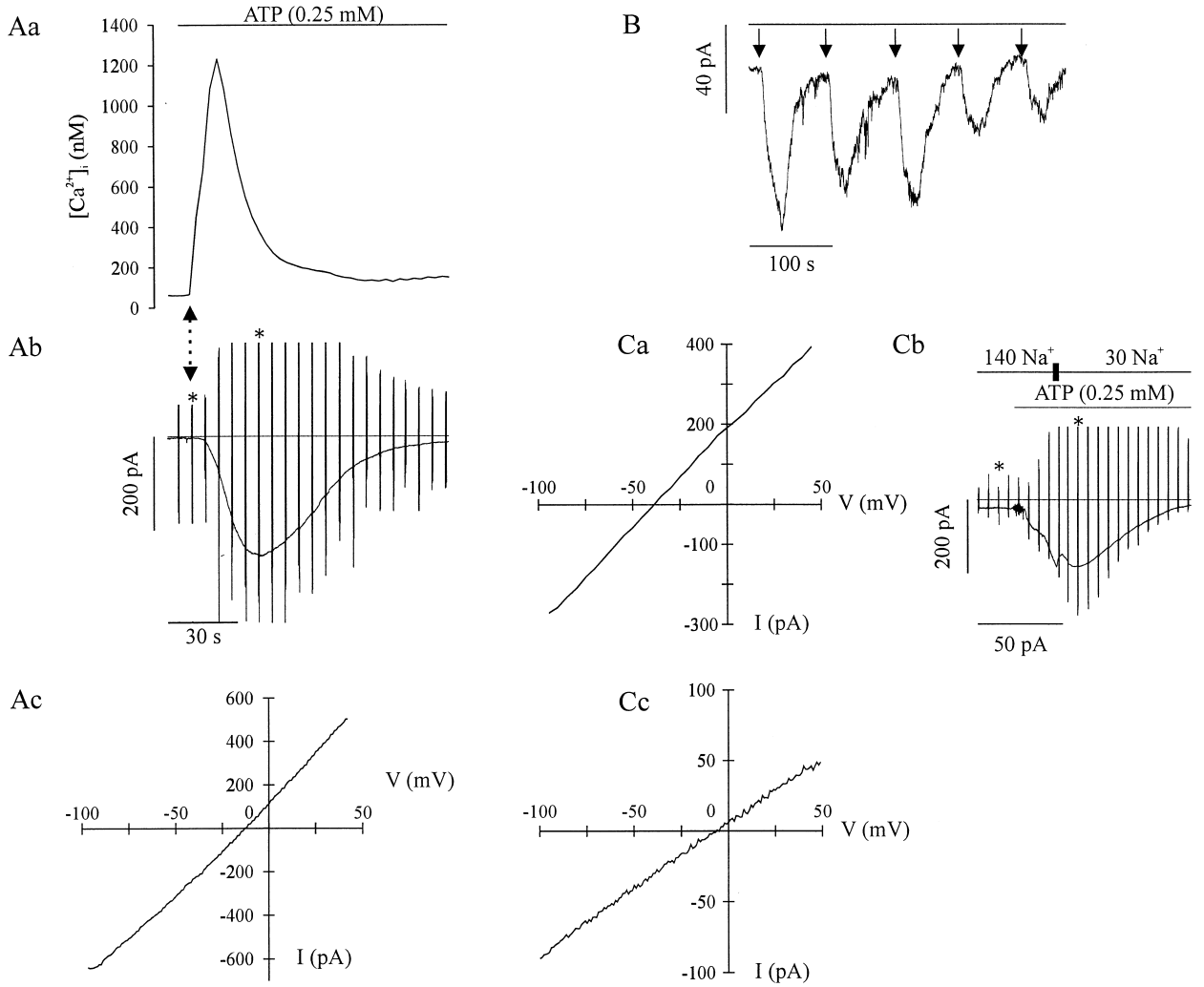

Fig. 2. ATP-mediated P2Y receptor activation evokes a non-selective cation current in human DC-14. Aa–Ac: Application of ATP (0.25 mM) through a puffer pipette led in a fura-2-AM loaded human DC to a transient $[Ca^{2+}]_i$ rise (Aa) and the activation of a slowly activating and inactivating inward current in the continuous presence of the agonist (perforated patch clamp technique, HP = −80 mV, Ab). Intermittently voltage ramps were applied (−100–50 mV, 150 ms, Ab). Subtraction of voltage ramps (marked with a star) in the presence and absence of ATP (Ab) yielded a linear *I/V* relationship for the ATP induced current with a reversal potential close to 0 mV (Ac). The parallel monitoring of Ca^{2+} and membrane currents also evidenced that the $[Ca^{2+}]_i$ rise initiated prior to the activation of the inward current (see also double arrow marking the beginning of the $[Ca^{2+}]_i$ increase, Ab). B: 1 s lasting ATP applications through a puffer pipette evoked in a voltage clamped DC (perforated patch-clamp configuration, HP = −80 mV) the slowly activating and inactivating inward current. Repetitive applications of ATP resulted in a decrease of the current amplitude indicating receptor desensitization. Ca–Cc: Isomolar replacement of extracellular Na^+ (110 mM) by NMDG caused a pronounced shift of the reversal potential to negative potentials (HP = −80 mV, subtracted voltage ramps are indicated with a star, Cb). Conversely, replacement of intracellular Cl^- by aspartate did not result in a change of the reversal potential (Cc), proving that the ATP-evoked current was of a non-selective nature.

in $[Ca^{2+}]_i$ preceded the activation of the current and the average delay between the onset of the rise in $[Ca^{2+}]_i$ and the activation of the current amounted to 2.9 ± 1.9 s ($n = 4$). The instantaneous *I/V* relationship was linear and yielded a reversal potential close to 0 mV (Fig. 2Ac, average value of −11.8 ± 0.5 mV for $n = 4$). ATP evoked this slowly activating and inactivating inward current at a holding potential (HP) of −80 mV in almost all DC-14 tested with an average amplitude of −276 ± 43 pA ($n = 23$). The current could be activated repetitively ($n = 2$), however, the amplitude decreased indicating receptor desensitization (Fig. 2B). To identify the nature of the current, ion replacement experiments were performed. Substitution of extracellular Na^+ by NMDG led in the instantaneous *I/V* relationships to a significant left shift (−49 ± 5 mV, $n = 2$) of the reversal potential (Fig. 2Ca/b). In contrast, replacement of extracellular or intracellular Cl^- by acetate or aspartate did not alter the reversal potential with values of −4.5 ± 2 mV ($n = 2$) and of −8.5 ± 2.5 mV ($n = 2$, Fig. 2Cc), respectively. These results demonstrate that P2Y receptor activation leads to the activation of a non-selective cation current. Since the increase in $[Ca^{2+}]_i$ was observed before the onset of the inward current (Fig. 2Aa/b), we investigated whether the current was Ca^{2+} activated. Therefore, DC-14 were dialyzed with 10 mM EGTA and 100 μM fura-2 to prevent ATP-induced $[Ca^{2+}]_i$ increase. As can be seen in Fig. 3Aa/b, ATP still activated the inward current 5 min after the establishment of the classic whole cell configuration (Fig. 3Ab), however, no concomitant elevation of $[Ca^{2+}]_i$ occurred

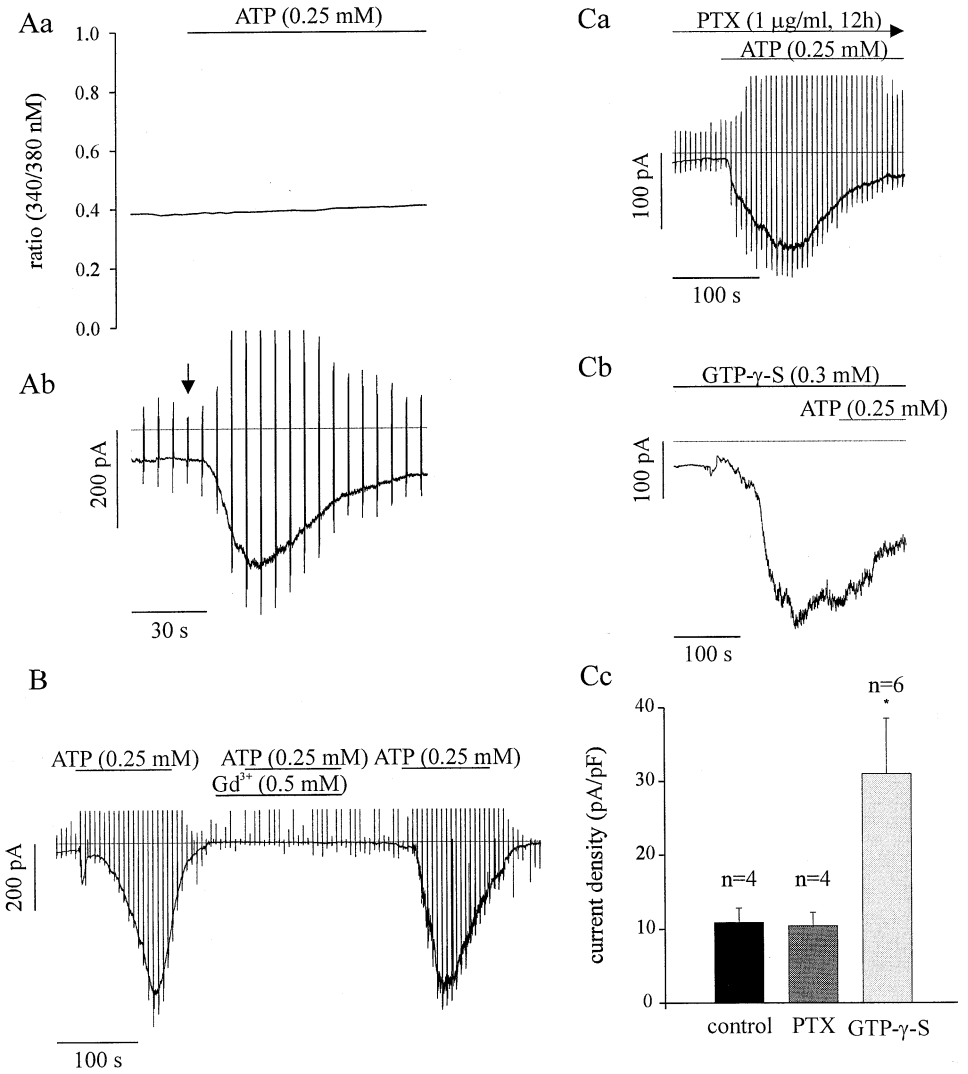

Fig. 3. Regulation of ATP evoked inward currents. Aa, Ab: Representative experiment where intracellular stores were Ca^{2+} depleted by dialyzing the cell via the patch pipette in the classic whole cell configuration with high concentrations of fura-acid (100 μM) and EGTA (10 mM) for 5 min. The subsequent application of ATP resulted in activation of the typical inward current (Ab), whereas no transient increase of the 340/380 ratio (Aa) was noted. This indicated that the ATP evoked current was not Ca^{2+} activated. B: The ATP evoked non selective cation current was inhibited by Gd^{3+} (0.5 mM, HP = −80 mV). Ca-Cc: ATP activated the inward current also in PTX preincubated DC-14, excluding the involvement of G proteins of the G_s/G_i type (Ca). Similarly, inclusion of GTP-γ-S (0.3 mM) in the patch pipette resulted in the activation of a non inactivating inward current (HP = −80 mV, Cb). Application of ATP after full establishment of the GTP-γ-S evoked inward current was without effect (Cb). The statistical significant difference of current densities evoked by ATP, in the presence of PTX and by GTP-γ-S is shown (Cc, unpaired Student's *t*-test < 0.01).

(Fig. 3Aa, $n = 8$). This was further confirmed, by experiments where the application of Tg did not result in current activation, whereas subsequently applied ATP evoked the characteristic inward current ($n = 4$, data not shown). We further investigated possible inhibitors of the ATP evoked non-selective cation current. While the P2X/P2Y receptor blocker suramin (100 μM) did not prevent current activation ($n = 2$, data not shown), Gd^{3+} (0.5 mM) completely blocked the ATP response (Fig. 3B, $n = 3$). An involvement of G proteins of the G_i/G_o subfamily in the activation of the current was also excluded since preincubation in PTX did not prevent current activation by ATP (Fig. 3Ca, $n = 4$). Because the inward current was not activated by Ca^{2+}, we tested whether G-protein activation was sufficient to evoke the current. Indeed, infusion of GTP-γ-S (300 μM), a permanent activator of all G-proteins resulted in the activation of a sustained inward current; subsequent application of ATP was without effect (Fig. 3Cb, $n = 4$), suggesting that the ATP- and GTP-γ-S activated currents were identical. The current density of the ATP evoked inward current (HP = −80 mV) was almost identical under control conditions and upon incubation in PTX (Fig. 3Cc). Conversely, the GTP-γ-S induced current density was significantly higher (Fig. 3Cc), probably due to the activation of all available G-proteins.

Because P2Y receptor activation shared identical signal transduction cascades as described for chemokine receptors [32], we analyzed whether any changes in the orientation of dendrites and cell shape could be observed in DC-14 upon site directed application of ATP. For this purpose a glass pipette containing high ATP concentration (1 mM) was placed in the recording chamber. Typically, over time a reorientation of dendrites and of cell shape towards the ATP containing pi-

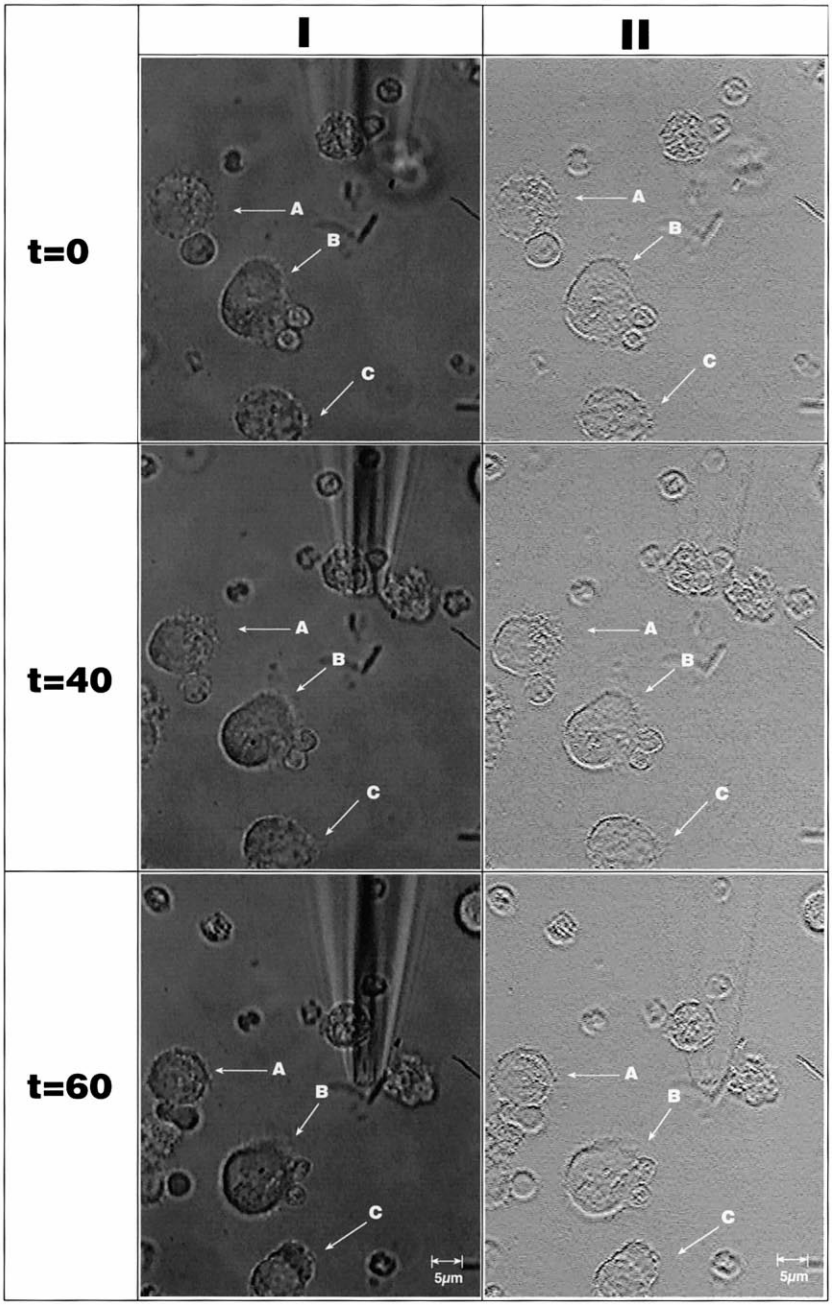

Fig. 4. Human DC-14 reorientate dendrites and cell shape towards an ATP containing pipette. The numbers on the left side indicate time points in min when pictures of the continuous video-sequence were taken for digitization. In order to show the changes occurring over time the original pictures displayed on the left side (I) are also displayed in the relief mode (II): Representative images of continuous video-microscopic monitoring of orientation of dendrites as well as of cell shape of DC-14 cells in vicinity of a glass pipette filled with normal extracellular solution containing 1 mM ATP. 40 min after positioning the pipette ($t=40$) the orientation of the dendrites as well as of cell shape (A, B and C) clearly changed as compared to the control picture acquired immediately prior to proper placement of the pipette ($t=0$). Further change of the pipette position (shortly after acquisition of $t=40$) resulted again in reorientation of dendrites as well as of cell shape towards the ATP containing pipette ($t=60$), excluding that the changes observed were a result of ATP toxicity. Calibration bar equals 5 μm.

pette was observed (as shown in the time lapse pictures in Fig. 4). Control experiments using normal extracellular solution instead of ATP did not result in similar changes (data not shown). When the pipette was repositioned, de novo reorientation of dendrites and of cell shape occurred (Fig. 4C), excluding that this could be related to a toxic effect of ATP.

Taken together we present evidence that human DC-14 express at least three subtypes of functionally coupled P2Y receptors but none of the P2X family. This is in clear contrast to human macrophages where the functional expression of P2X receptors was described [15,33]. Interestingly, P2Y receptor activation leads to a transient rise of $[Ca^{2+}]_i$ and a concomitant activation of a non-selective cation current. Although in rat macrophages ATP evoked a non-selective cation current [34,35], the receptors involved were of the P2X7 subtype and the biophysical characteristics of the currents differed from our findings in CD14-derived DCs primarily by the slow activation kinetics and the inactivation in

presence of ATP. Because of the similarity between the P2Y and chemokine receptor coupling the effect of ATP on DCs was tested. We demonstrate, to our knowledge for the first time, that local ATP application leads to reorientation of dendrites and changes of cell shape. Because of the reorientation of DC-14 after the position change of the application pipette and the lack of P2X7 expression on human DC-14, ATP induced cell lysis can be excluded [36]. Our observations imply a novel role for P2Y receptors as possible chemokine receptors. Since within inflammatory sites infected or dying cells are likely to release ATP, this mechanism may serve as an important stimulus for redirecting DCs to entry sites of pathogens.

Future studies should be directed to clarify this in more detail using classic cell migration assays as well as various pharmacological agents (ATP, Gd^{3+}, etc.). Moreover, the functional role of the transient $[Ca^{2+}]_i$ increase and the non-selective cation current has to be further investigated.

References

[1] Banchereau, J. and Steinman, R.M. (1998) Nature 392, 245–252.
[2] Celluzzi, C.M., Mayordomo, J.I., Storkus, W.J., Lotze, M.T. and Falo, L.D.J. (1996) J. Exp. Med. 183, 283–287.
[3] Bender, A., Bui, L.K., Feldman, M.A., Larsson, M. and Bhardwaj, N. (1995) J. Exp. Med. 182, 1663–1671.
[4] Serwe, M., Reuter, G., Sponaas, A., Koch, S. and Koch, N. (1997) Int. Immunol. 9, 983–991.
[5] Koch, F., Trockenbacher, B., Kampgen, E., Grauer, O., Stossel, H., Livingstone, A.M., Schuler, G. and Romani, N. (1995) J. Immunol. 155, 93–100.
[6] Nijman, H.W., Kleijmeer, M.J., Ossevoort, M.A., Oorschot, V.M., Vierboom, M.P., van de Keur, M., Kenemans, P., Kast, W.M., Geuze, H.J. and Melief, C.J. (1995) J. Exp. Med. 182, 163–174.
[7] Coughlan, S.N., Harkiss, G.D., Dickson, L. and Hopkins, J. (1996) Scand. J. Immunol. 43, 31–38.
[8] Sallusto, F. and Lanzavecchia, A. (1994) J. Exp. Med. 179, 1109–1118.
[9] Bujdoso, R., Harkiss, G., Hopkins, J. and McConnell, I. (1990) Int. Rev. Immunol. 6, 177–186.
[10] Burnstock, G. (1996) Ciba Found. Symp. 198, 1–28.
[11] North, R.A. and Barnard, E.A. (1997) Curr. Opin. Neurobiol. 7, 346–357.
[12] Ross, P.E., Ehring, G.R. and Cahalan, M.D. (1997) J. Cell Biol. 138, 987–998.
[13] Baricordi, O.R., Ferrari, D., Melchiorri, L., Chiozzi, P., Hanau, S., Chiari, E., Rubini, M. and Di Virgilio, F. (1996) Blood 87, 682–690.
[14] Di Virgilio, F., Ferrari, D., Falzoni, S., Chiozzi, P., Munerati, M., Steinberg, T.H. and Baricordi, O.R. (1996) Ciba Found. Symp. 198, 290–302.
[15] Falzoni, S., Munerati, M., Ferrari, D., Spisani, S., Moretti, S. and Di Virgilio, F. (1995) J. Clin. Invest. 95, 1207–1216.
[16] Chused, T.M., Apasov, S. and Sitkovsky, M. (1996) J. Immunol. 157, 1371–1380.
[17] Ferrari, D., Munerati, M., Melchiorri, L., Hanau, S., Di Virgilio, F. and Baricordi, O.R. (1994) Am. J. Physiol. 267, C886–892.
[18] Grynkiewicz, G., Poenie, M. and Tsien, R.Y. (1985) J. Biol. Chem. 260, 3440–3450.
[19] Hamill, O.P., Marty, A., Neher, E., Sakmann, B. and Sigworth, F.J. (1981) Pflugers Arch. 391, 85–100.
[20] Korn, S.J. and Horn, R. (1989) J. Gen. Physiol. 94, 789–812.
[21] Fischer, H.G. and Eder, C. (1995) FEBS Lett. 373, 127–130.
[22] Thastrup, O., Cullen, P.J., Drobak, B.K., Hanley, M.R. and Dawson, A.P. (1990) Proc. Natl. Acad. Sci. USA 87, 2466–2470.
[23] Ross, P.E., Garber, S.S. and Cahalan, M.D. (1994) Biophys. J. 66, 169–178.
[24] Pintor, J., King, B.F., Miras-Portugal, M.T. and Burnstock, G. (1996) Br. J. Pharmacol. 119, 1006–1012.
[25] Tokuyama, Y., Fan, Z., Furuta, H., Makielski, J.C., Polonsky, K.S., Bell, G.I. and Yano, H. (1996) Biochem. Biophys. Res. Commun. 220, 532–538.
[26] Schachter, J.B., Li, Q., Boyer, J.L., Nicholas, R.A. and Harden, T.K. (1996) Br. J. Pharmacol. 118, 167–173.
[27] Janssens, R., Communi, D., Pirotton, S., Samson, M., Parmentier, M. and Boeynaems, J.M. (1996) Biochem. Biophys. Res. Commun. 221, 588–593.
[28] Lustig, K.D., Shiau, A.K., Brake, A.J. and Julius, D. (1993) Proc. Natl. Acad. Sci. USA 90, 5113–5117.
[29] Parr, C.E., Sullivan, D.M., Paradiso, A.M., Lazarowski, E.R., Burch, L.H., Olsen, J.C., Erb, L., Weisman, G.A., Boucher, R.C. and Turner, J.T. (1994) Proc. Natl. Acad. Sci. USA 91, 3275–3279.
[30] Communi, D., Pirotton, S., Parmentier, M. and Boeynaems, J.M. (1995) J. Biol. Chem. 270, 30849–30852.
[31] Nguyen, T., Erb, L., Weisman, G.A., Marchese, A., Heng, H.H., Garrad, R.C., George, S.R., Turner, J.T. and O'Dowd, B.F. (1995) J. Biol. Chem. 270, 30845–30848.
[32] Baggiolini, M., Dewald, B. and Moser, B. (1997) Annu. Rev. Immunol. 15, 675–705.
[33] Chiozzi, P., Sanz, J.M., Ferrari, D., Falzoni, S., Aleotti, A., Buell, G.N., Collo, G. and Di Virgilio, F. (1997) J. Cell Biol. 138, 697–706.
[34] Naumov, A.P., Kaznacheyeva, E.V., Kiselyov, K.I., Kuryshev, Y.A., Mamin, A.G. and Mozhayeva, G.N. (1995) J. Physiol. (Lond.) 486, 323–337.
[35] Naumov, A.P., Kiselyov, K.I., Mamin, A.G., Kaznacheyeva, E.V., Kuryshev, Y.A. and Mozhayeva, G.N. (1995) J. Physiol. (Lond.) 486, 339–347.
[36] Chiozzi, P., Murgia, M., Falzoni, S., Ferrari, D. and Di Virgilio, F. (1996) Biochem. Biophys. Res. Commun. 218, 176–181.